

Design of a Smooth Landing Trajectory Tracking System for a Fixed-wing Aircraft

Solomon Gudeta and Ali Karimodini

Abstract—This paper presents a landing controller for a fixed-wing aircraft during the landing phase, ensuring the aircraft reaches the touchdown point smoothly. The landing problem is converted to a finite-time linear quadratic tracking (LQT) problem in which an aircraft needs to track desired landing path in the longitudinal-vertical plane while satisfying performance requirements and flight constraints. First, we design a smooth trajectory that meets flight performance requirements and constraints. Then, an optimal controller is designed to minimize the tracking error, while landing the aircraft within the desired time-frame. For this purpose, a linearized model of an aircraft developed used under the assumption of a constant approach airspeed, is used. The resulting Differential Riccati equation is solved backward in time using the Dormand Prince algorithm. Simulation results show a good tracking performance and the finite-time convergence of tracking errors for different initial conditions of the flare-out phase of landing.

I. INTRODUCTION

One of the most difficult tasks in aircraft control is achieving a safe and comfortable landing. A review of accident statistics indicates that over 45 percent of all general aviation accidents occur during the approach and landing phases of a flight [1]. A closer look shows that the cause of over 90 percent of those cases was pilot related. Loss of control was also a major contributing factor in 33 percent of these cases. In many cases, the accidents have happened due to not landing within a targeted landing time [2]. Aircraft landing has five phases: the base leg, the glide slope, the flare-out, the touchdown, and the after-landing roll. The glide slope and the flare-out are the most crucial phases. In the glide slope phase the aircraft descends along a predefined straight line at a steady state descent angle; whereas, in the flare-out phase the aircraft gradually raises its nose while landing. There are several performance requirements and constraints associated with aircraft landing. The aircraft needs to follow the desired trajectory and land smoothly within a targeted landing time. In addition, the aircraft landing controller should be robust to wind turbulence, measurement noise, and actuator failures.

Many researchers have applied various control techniques to design an automatic aircraft landing control system. Different control methods such as classical control [3], [4], optimal control [2], [5]–[7], adaptive control [8], [9], nonlinear control [10], [11], and intelligent control [12]–[14] have been used to solve the automatic aircraft landing

problem. In [15], the flare-out maneuver control was successfully implemented using the classical feedback control method. [3] implemented a PID controller combined with an evolutionary technique to tune control gains. Generally, classical controllers often lack optimality in achieving desired performances. [2] applied an optimization technique called the parametric expansion method to synthesize a linear time-varying aircraft landing controller. In [5], [13], [16]–[18] issues such as robustness to measurement noise, actuator faults, wind disturbances, and flight uncertainties were investigated and H_2 , H_∞ , LQR/LQG, mixed H_2/H_∞ control techniques were employed to design optimal and robust aircraft landing controllers. Recently, concepts from adaptive control and intelligent control such as adaptive synthesis based on dynamic inversion theory [10], [13], [19], neural networks [14], quantitative feedback theory [9], sliding mode control [8], structured singular value μ -synthesis, or fuzzy techniques [20] were used to design automatic aircraft landing controllers. In [8], [11], [18] nonlinear control techniques were applied to improve the control performance of the landing controller. Most of the aforementioned techniques are based on the asymptotic convergence of tracking errors. This does not guarantee a safe, smooth, and comfortable landing, which often requires the aircraft to accurately track a particular landing profile while landing within a given period of time and satisfying performance requirements and flight constraints.

The contribution of this paper is, therefore, designing an optimal controller that guarantees the finite-time convergence of the landing trajectory tracking errors. For this purpose, we first design the desired landing path which satisfies performance requirements and flight constraints. The flare-out maneuver phase is designed as an exponential path, which connects end point of glide slope phase and the touchdown point on the runway. Furthermore, the touchdown point is captured as a boundary condition. In addition, performance requirements and constraints on control input and output signals are determined. Subsequently, we formulate the tracking problem by designing a performance index which should be minimized in a targeted landing time. We then have converted the aircraft landing problem to a Linear Quadratic Tracking (LQT) problem where we minimize the designed cost function for a linear model of the aircraft respecting boundary conditions. Control gains are found by solving differential Riccati equations backward in time using the Dormand Prince algorithm. The simulation results are analyzed to show that the developed trajectory tracking system can handle a range of angle of attack and headwind

S. G. Gudeta and A. Karimodini are with the Department of Electrical and Computer Engineering, North Carolina Agricultural and Technical State University, Greensboro, North Carolina, USA.

Corresponding author: A. Karimodini, Tel: +13362853313, akarimod@ncat.edu.

disturbances.

In the remainder of this paper, in Section II, the aircraft landing problem is formulated. In Section III, the desired trajectory and performance index are designed by incorporating the performance requirements and flight constraints. An LQT controller is developed for aircraft landing by minimizing the designed performance index to guide the aircraft to follow the desired landing trajectory. In Section IV, the proposed flight controller is simulated and the results are discussed. Finally, Section V concludes this paper.

II. PROBLEM FORMULATION

The aircraft landing process is described in Figure 1. The glide slope phase and flare-out phase are the most critical steps. After the base leg, the aircraft should descend towards the runway center-line with the flight path angle ν between 2.5 to 3.5 deg. As the aircraft descends to a certain altitude above the ground, the *flare-out* phase begins. In the *flare-out* phase of landing, the pitch angle θ of the airplane must be gradually adjusted to have a value between 0 to 10 deg, and the aircraft should approach the touchdown point smoothly. The flare-out phase is the most difficult part of the landing maneuver, as the run-way is not in the pilot's field of view and the touchdown point has to be accurately reached within a targeted time smoothly, following the landing trajectory. In this paper, we assume that the lateral and longitudinal dynamics of the aircraft are decoupled, and the lateral controller [21] takes care of the lateral deviations from the center line of the runway. The focus of this paper, therefore, is on the design of a longitudinal controller to track the desired landing trajectory. The longitudinal motion of the

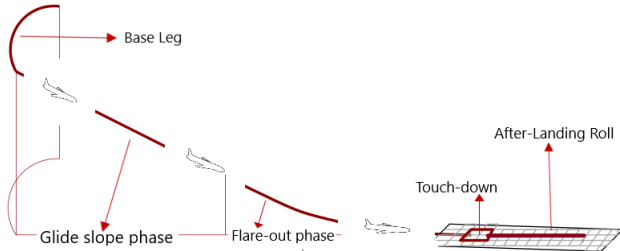


Fig. 1: An aircraft landing phases: the base leg, the glide slope, the flare-out, the touchdown, and the after-landing roll.

aircraft is governed entirely by the elevator deflection angle $\delta_e(t)$. The longitudinal dynamics of an aircraft is given by the so-called short period equation of motion [2] of the aircraft:

$$\dot{\theta}(s) = \frac{K_s(T_s s + 1)}{\left(\frac{s^2}{\omega_s^2} + \frac{2\zeta s}{\omega_s} + 1\right)} \delta_e(s) \quad (1)$$

where $\dot{\theta}$ is pitch rate, K_s is short period gain, T_s is path time constant, ω_s is short period resonant frequency, and ζ is short period damping factor. Assuming the velocity V of the aircraft to be constant, pitch angle rate $\dot{\theta}$ and altitude h are related [2] through vertical acceleration \ddot{h} as:

$$\ddot{h}(s) = \frac{V}{T_s s + 1} \dot{\theta}(s) \quad (2)$$

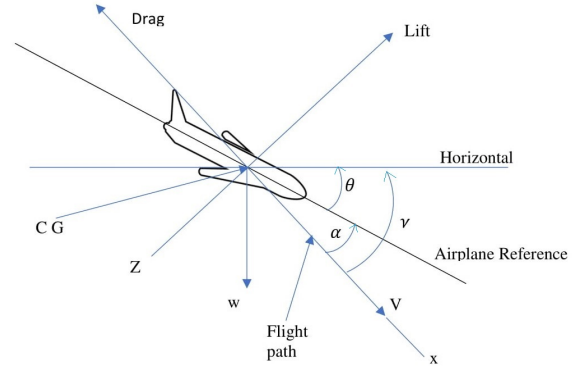


Fig. 2: Definition of aircraft coordinates and angles [2]. α is the angle of attack, θ is the pitch angle, ν is the flight path angle.

Combining (1) and (2), a fourth-order linear differential equation is found:

$$h^{(4)}(t) + 2\zeta\omega_s h^{(3)}(t) + \omega_s^2 \ddot{h}(t) = K_s V \omega_s^2 \delta_e(t) \quad (3)$$

Substituting

$$\ddot{h}(t) = \frac{V}{T_s} \dot{\theta}(t) - \frac{1}{T_s} \dot{h}(t), h^{(3)}(t) = \frac{V}{T_s} \ddot{\theta}(t) - \frac{1}{T_s} \ddot{h}(t) \quad (4a)$$

$$h^{(4)}(t) = \frac{V}{T_s} \ddot{\theta}(t) - \frac{1}{T_s} \ddot{h}^{(3)}(t) \quad (4b)$$

in (3), the new aircraft equation of motion becomes

$$\begin{aligned} & \frac{V}{T_s} \ddot{\theta}(t) - \left(\frac{V}{T_s^2} - 2\zeta\omega_s \frac{V}{T_s}\right) \dot{\theta}(t) - \left(2\zeta\omega_s \frac{V}{T_s^2} - \omega_s^2 \frac{V}{T_s^2} \right. \\ & \left. - \frac{V}{T_s^3}\right) \theta(t) - \left(\frac{1}{T_s^3} - 2\zeta\omega_s \frac{1}{T_s^2} + \frac{\omega_s^2}{T_s}\right) \dot{h}(t) = K_s V \omega_s^2 \delta_e(t) \end{aligned} \quad (5)$$

from which one can derive, the state space representation of the aircraft's model as:

$$\dot{x}(t) = Ax(t) + B\delta_e(t) \quad (6a)$$

$$y = Cx(t) \quad (6b)$$

where $x(t) = [h(t) \dot{h}(t) \theta(t) \dot{\theta}(t)]^T$, $B = [0 \ 0 \ 0 \ b_4]^T$,

$$A = \begin{bmatrix} 0 & 1 & 0 & 0 \\ 0 & a_{22} & a_{23} & 0 \\ 0 & 0 & 0 & 1 \\ 0 & a_{42} & a_{43} & a_{44} \end{bmatrix}, \quad a_{22} = -\frac{1}{T_s}, \quad a_{23} = \frac{V}{T_s}, \quad a_{42} = \frac{1}{vT_s^2} - 2\zeta\omega_s \frac{V}{T_s^2} + \frac{\omega_s^2}{V}, \quad a_{43} = 2\zeta\omega_s \frac{1}{T_s^2} - \omega_s^2 - \frac{1}{T_s^2}, \quad a_{44} = \frac{1}{T_s} - 2\zeta\omega_s, \quad b_4 = \omega_s^2 K_s T_s \text{ and } C \text{ is the identity matrix.}$$

Our aim is to design a controller for the aircraft to follow the landing trajectory with the minimum tracking error $e(t)$ given as:

$$e(t) = x(t) - r(t) \quad (7)$$

where $r(t) \in \mathbb{R}^4$ is the desired landing trajectory over the landing time interval $[t_0, t_f]$. Then, given an aircraft model in (6) and boundary conditions as $x(t_0) = x_0$ and $x(t_f) = x_f$, we address the following problems for the aircraft landing:

Problem 1: Design a desired landing flight trajectory $r(t)$ which captures performance requirements and flight constraints.

Problem 2: Design a performance index J to capture performance requirements and constraints

Problem 3: Design a controller that tracks the desired trajectory $r(t)$ and satisfies the given performance requirements and constraints.

III. LANDING TRAJECTORY TRACKING

A. Trajectory design

The aircraft landing trajectory is the desired aircraft landing path, which the aircraft follows over a specified period of time $[t_0, t_f]$. Landing trajectory must ensure safe and comfortable landing. The desired landing path is expressed as a desired altitude which is a function of forward distance. Its important phases are the glide slope phase and flare-out phase as shown in Figure 3. The glide slope phase is the first part of a landing path. It is modeled as a straight line path whose slope is given in terms of the flight path angle ν . The other part is the flare-out path which is initiated when the aircraft reaches to a certain height h_{f_0} above the landing surface. Flare-out path is an exponential path with a near zero flight path angle at touchdown. In Figure 3, the desired landing path is shown in forward distance (X)-altitude (h)-plane.

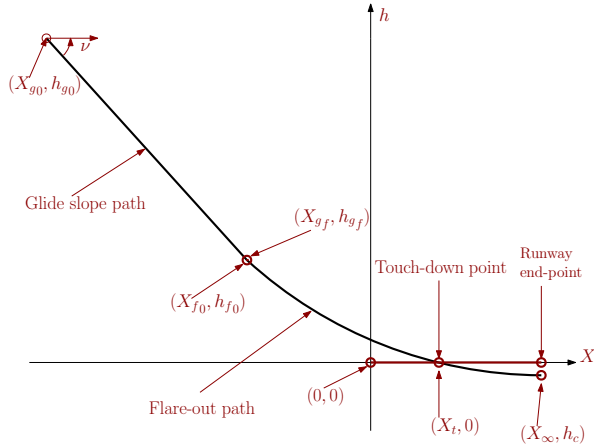


Fig. 3: An aircraft landing path where (X_{g_0}, h_{g_0}) and (X_{g_f}, h_{g_f}) are the beginning and the endpoint of the glide slope path; (X_{f_0}, h_{f_0}) and $(X_t, 0)$ are the beginning and the endpoint of the flare-out path; $(0, 0)$ is the origin of X-h plane, and (X_{∞}, h_c) is the final point on the flare-out path usually defined below the ground. The origin of the X-h plane is assumed to be at the beginning of the runway and the aircraft must land within one-third of the runway.

In the glide slope phase the aircraft tracks a straight line path pointing toward the beginning of the runway. The desired altitude, h^d , is computed based on a given flight path angle ν :

$$h^d = -\tan(\nu^d)(X - X_{g_0}) + h_{g_0} \quad (8)$$

As soon as the flare-out phase starts, the desired altitude h^d is computed as:

$$h^d = -h_c + (h_{f_0} + h_c)e^{-K_x(X - X_{f_0})} \quad (9)$$

where K_x is a constant which defines the curvature of flare-out maneuver path, depending on the distance between the origin of X-h plane and the touchdown point.

The objective of a good, stabilized final approach is to descend at an angle and airspeed that permits the airplane to reach the desired touchdown point with minimum floating; in essence, a semi-stalled condition [1]. To accomplish this, it is essential that both the descent angle and the airspeed be

accurately controlled. Since on a normal approach the power setting is not fixed as in a power-off approach, the power and pitch attitude are adjusted simultaneously as necessary to control the airspeed and the descent angle, or to attain the desired altitudes along the approach path. In this paper, we focus on the flare-out phase to achieve a safe and comfortable landing. In (9), X_{f_0} , h_c and K_x are unknowns. We can solve for these unknowns from $\tan(\nu^d)$, h_{f_0} , and X_t under the following constraints:

- Slope continuity constraint: For a smooth phase change, the slope at the beginning of the flare-out path should be equal to the slope of the glide slope path. Thus, the slope of glide slope path can be calculated as

$$\dot{h}^d = -\tan(\nu^d) \quad (10)$$

Similarly, the slope at the beginning of flare-out path is

$$\dot{h}^d = -K_x(h_{f_0} + h_c)e^{-K_x(X - X_{f_0})}|_{X=X_{f_0}} \quad (11)$$

Using (10) and (11), K_x is computed as

$$K_x = \frac{\tan(\nu^d)}{h_{f_0} + h_c} \quad (12)$$

- Path continuity constraint: This constraint guarantees the continuity of the path when transiting from the glide slope phase to the flare-out phase. By design, we have $X_{f_0} = X_{g_f}$. We then need to ensure that h^d at X_{g_f} given in (8) is the same as h^d at X_{f_0} given in (9) resulting in

$$X_{f_0} = \frac{h_{g_0} - h_{f_0}}{\tan(\nu^d)} + X_{g_0} \quad (13)$$

- Touchdown constraint: The landing path intersects the ground at the touchdown point X_t . Thus, at touchdown point we have

$$-h_c + (h_{f_0} + h_c)e^{-K_x(X_t - X_{f_0})} = 0 \quad (14)$$

Finally, K_x and h_c are found by solving (12), (13) and (14).

Under the assumption of constant aircraft forward velocity \dot{X} , at any time moment $t > t_0$, the forward distance X on the flare-out curve will be approximately

$$X = X_{f_0} + \dot{X}(t - t_0) \quad (15)$$

Substituting $X - X_{f_0}$ from (15) in (9), the landing trajectory in flare-out phase is governed by

$$h^d = -h_c + (h_{f_0} + h_c)e^{-K(t - t_0)} \quad (16)$$

where $K = K_x \dot{X}$. By differentiating (16), the desired rate of descent in flare-out phase is:

$$\dot{h}^d = -K(h_{f_0} + h_c)e^{-K(t - t_0)} \quad (17)$$

The value of the pitch angle is crucial only during the last few sec of landing before the touchdown point. In flare-out maneuver phase, the desired pitch angle, θ_d , is::

$$\theta_d = 0 \quad (18)$$

Also, for a safe and comfortable landing, the pitch rate $\dot{\theta}_d$ should be:

$$\dot{\theta}_d = 0 \quad (19)$$

B. Performance requirements

The following landing requirements and flight constraints are considered for the aircraft landing in this paper:

- C1: The landing path should be an exponential path such that it ensures a safe and comfortable landing.
- C2: The rate of descent \dot{h} should be non-zero in order to avoid overshooting. In addition, the rate of descent at touchdown should be a small negative value in order to prevent over stressing of landing gear. Requirements to avoid undesirable behaviors such as landing gear over stress, aircraft floating down runway and aircraft overshooting runway are captured by magnitude of rate of descent at touchdown point. Typically based on type of the aircraft, a value between 60 to 180 ft/min is considered as an ideal rate of descent at touchdown point.
- C3: The lower limit on the pitch angle θ should be 0° in order to prevent the nose wheel of an aircraft from touching down first, and the upper limit on the pitch angle θ should be 10° to prevent the tail gear from touching down first.
- C4: During landing, in the flare-out maneuver phase, the angle of attack must remain below 80 percent of the stall value. The stall value is assumed to be 18° [2]. Hence, the rate of change of angle attack is restricted to a value less than 20 percent of the stall value:
- C5: The longitudinal motion control is mainly executed by the elevator. To avoid saturation, the elevator is not permitted to operate against the mechanical stops during the landing process. Thus, the deflection of the elevator is restricted between -35° and $+15^\circ$.

In addition, the aircraft should follow the designed landing trajectory and reduce the tracking error within the targeted landing time t_f with minimum control effort $\delta_e(t)$. This can be captured by the following performance index:

$$J = [Cx(t_f) - r(t_f)]^T P [Cx(t_f) - r(t_f)] + \int_{t_0}^{t_f} \{ [Cx(\tau) - r(\tau)]^T Q [Cx(\tau) - r(\tau)] + \delta_e^T(\tau) R \delta_e(\tau) \} d\tau \quad (20)$$

where $P \geq 0$, $Q \geq 0$, $R > 0$, are all symmetric weighting parameters. The terms outside the integral ensure that the states are close to the desired values at the touchdown point, avoiding an early or a late landing. On the other hand, the terms inside the integral push the aircraft to track the desired landing trajectory with minimum control effort in the landing time $[t_0, t_f]$.

C. Controller design based on linear quadratic tracking

Given the aircraft model in (6) and the boundary conditions $x(t_0) = x_0 = [h(t_0)=h_{f0} \ \dot{h}(t_0) \ \theta(t_0) \ \dot{\theta}(t_0)]^T$ and $x(t_f) = x_f = [0 \ 0 \ 0 \ 0]^T$, our aim is to find an optimal control $\delta_e^*(t)$ that guides the aircraft to follow the desired landing trajectory $r(t)$ over the time interval $[t_0, t_f]$, minimizing the performance index in (20), as described below:

$$\min_{\forall t \in [t_0, t_f]} J \quad (21)$$

subject to

$$\begin{cases} \dot{x}(t) = Ax(t) + B\delta_e(t) \\ x(t_0) = x_0 \\ x(t_f) = x_f \end{cases}$$

Defining the co-state vector $\lambda(t) = S(t)x(t) - v(t)$, where $S(t) = C^T P(t) C(t)$ and $v(t) = C^T P r(t)$, and defining the Hamiltonian function $H = \frac{1}{2} [Cx(t) - r(t)]^T Q [Cx(t) - r(t)] + \frac{1}{2} \delta_e^T(t) R \delta_e(t) + \lambda^T (Ax(t) + B\delta_e(t))$, the constrained optimization in (21) will be converted to

$$\min_{\forall t \in [t_0, t_f]} \bar{J} = [Cx(t_f) - r(t_f)]^T P [Cx(t_f) - r(t_f)] + \int_{t_0}^{t_f} (H - \lambda^T \dot{x}(t)) d\tau \quad (22)$$

whose solution can be found from $\delta J(x(t)) = 0$, where δJ is the variation of the functional J . The optimal control function will be

$$\delta_e^*(t) = -K(t)x(t) + R^{-1}B^T v(t) \quad (23a)$$

$$K(t) = R^{-1}B^T S(t) \quad (23b)$$

in which $S(t)$ and $v(t)$ can be found by solving the following differential equations in a backward way with a given boundary conditions:

$$-\dot{S} = A^T S + SA - SBR^{-1}B^T S + C^T QC \quad (24a)$$

$$-\dot{v} = (A - BK)^T v + C^T Q r \quad (24b)$$

$$S(t_f) = C^T P C \quad (24c)$$

$$v(t_f) = C^T P r(t_f) \quad (24d)$$

IV. SIMULATION

A simulation environment is set up by integrating the MATLAB and FlightGear simulation Software in which we simulated an aircraft landing from the altitude of 95 ft to the runway 10L of San Francisco airport. The information on the approach plate (see Table II) of runway 10L of the airport is used to design a safe and comfortable landing trajectory for an aircraft with model parameters given in Table I. Table II summarizes parameters extracted from the approach plate. Similarly, assuming this particular aircraft has a nominal initial altitude h_{f0} of 100 ft, the desired flight path angle ν of 3 deg, and the pitch angle θ of 0 deg, then using (12) to (15), we found the desired landing trajectory parameters X_{f0} , K_x , h_c , K , as shown in Table III.

The designed desired landing trajectory is plotted in Figure 4 in solid blue. The desired altitude $h^d(t)$ and the desired altitude rate $\dot{h}^d(t)$ are exponential functions while the desired pitch angle θ_d and the desired pitch rate $\dot{\theta}_d$ are constant functions. Both exponential functions and constant functions have derivatives of all orders. Therefore, the designed landing trajectory is a smooth landing trajectory.

N_0	Symbol	Parameter value
1	K_s	-0.95 sec^{-1}
2	T_s	40 sec
3	ω_s	1 rad/sec
4	ζ	0.5

TABLE I: The aircraft model parameters

$$P = \begin{bmatrix} 0.9 & 0 & 0 & 0 \\ 0 & 0.01 & 0 & 0 \\ 0 & 0 & 1 & 0 \\ 0 & 0 & 0 & 1 \end{bmatrix} \quad Q = \begin{bmatrix} 0.00067 & 0 & 0 & 0 \\ 0 & 0.0265 & 0 & 0 \\ 0 & 0 & 150 & 0 \\ 0 & 0 & 0 & 65 \end{bmatrix} \quad R = 1 \quad (25)$$

N_0	Name	Parameter value
1	X_{g0}	-34346 ft
2	h_{g0}	1800 ft
3	X_t	3957 ft

TABLE II: Parameters extracted from the approach plate

N_0	Name	Parameter value
1	K_x	0.00049
2	\dot{X}	256 ft/sec
3	K	0.1385
4	h_c	6.68 ft
5	X_{f0}	-1908 ft

TABLE III: The designed landing trajectory parameters

N_0	Parameter Name	Parameter value
1	t_0	0 sec
2	t_f	20 sec
3	h_0	95 ft
4	\dot{h}_0	-14 ft/sec
5	θ_0	-0.05 rad
6	$\dot{\theta}_0$	0 rad/sec
7	h_f	0 ft
8	\dot{h}_f	0 ft/sec
9	θ_f	0 rad
10	$\dot{\theta}_f$	0 rad/sec

TABLE IV: Simulation parameters: Initial and final conditions for case I

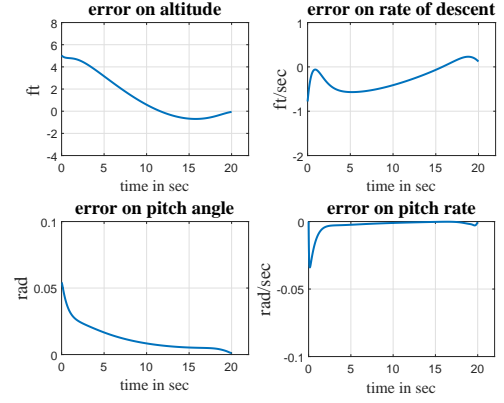


Fig. 5: The trajectory tracking error for the flight simulation results in Fig. 4

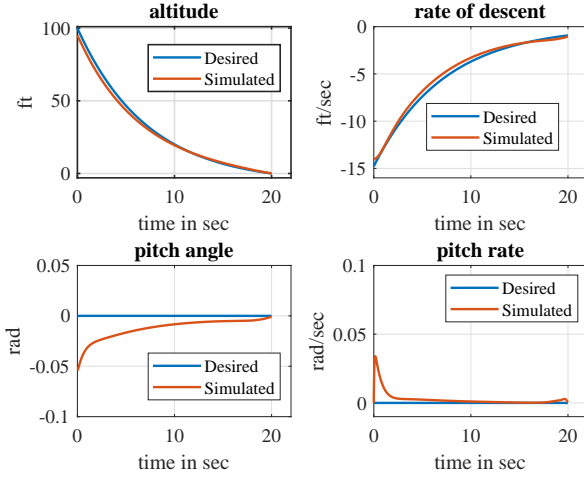


Fig. 4: The desired smooth landing trajectories (solid blue) and the simulated aircraft landing trajectories (solid red).

A. Case I: Simulation results for the initial condition given in Table IV

For the given initial conditions in Table IV, the simulated aircraft landing trajectory is shown in Figure 4 in red. The controller gain is found solving (24d) in a backward way using the Dormand-Prince algorithm. To respect the Constrains C1-C5 in Section III-B, we have tuned the performance index parameters R , Q , and P to values in (25). Comparing the desired altitude $h^d(t)$, the desired altitude rate $\dot{h}^d(t)$, and their respective simulation values in Figure 4, we can see that the aircraft has accurately tracked the desired landing trajectory in a desired landing time of 20 sec satisfying Constraints C1-C5 in Section III-B. This comparison is summarized in Table V.

B. Case II: Simulation results for different initial conditions

Head wind and deviation of a desired flight path angle from a desired value of 3 deg introduces a deviation in the gliding distance and the pitch angle which in turn give rise to a deviation in the initial altitude of the flare-out phase as shown in Figure 7. However, the designed controller can handle

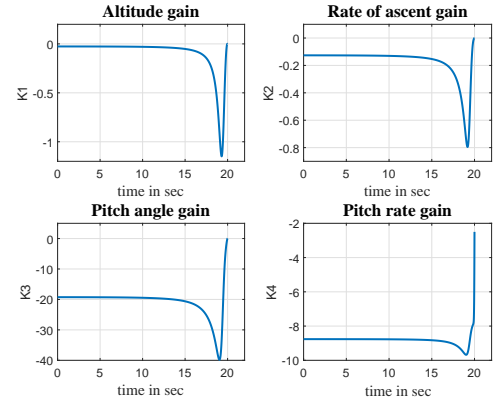


Fig. 6: Optimal controller gains for the flight simulation results in Fig. 4

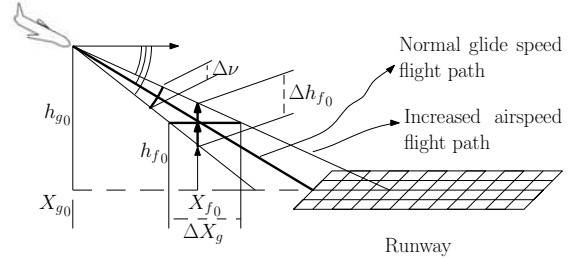


Fig. 7: The deviations in the gliding distance and the pitch angle due to head wind disturbances cause deviations in the initial altitude of the flare-out phase.

these deviations in the initial altitude Δh_{f0} and pitch angle $\Delta \theta$ by adjusting control input in order to maintain the rate of descent and the desired approach airspeed, while avoiding the saturation region of the elevator actuator (Constraint C5). Acceptable deviations in the initial altitude and pitch angle around the desired landing trajectory is determined by varying them correlationally until the control limiting values are attained instantaneously. Accordingly, Δh_{f0} and $\Delta \theta$ are found to be 20 ft and 1 deg respectively, and the corresponding region of operation is shown in Figure 8 in green.

N_0	Constraint	Constraint validation based on simulated flight data
C1	Exponential (smooth) trajectory	Satisfied by design in (9)
C2	$60 \leq \ h^d(t_f)\ \leq 180 \text{ ft/min}$	$\ h^d(t_f)\ = 62.7 \text{ ft/min}$
C3	$0^\circ \leq \theta(t_f) \leq +10^\circ$	$\theta(t_f) \approx 0$
C4	$\alpha(t) < 18^\circ$ $\Delta\alpha(t) < 3.6^\circ$	Satisfied through $\theta \approx 0$ and $\dot{\theta} \approx 0$
C5	$-35^\circ \leq \delta_e(t) \leq +15^\circ$	$-22.3^\circ \leq \delta_e(t) \leq +2.4^\circ$

TABLE V: Landing constraints C1-C5 validation for the given initial conditions in Table IV

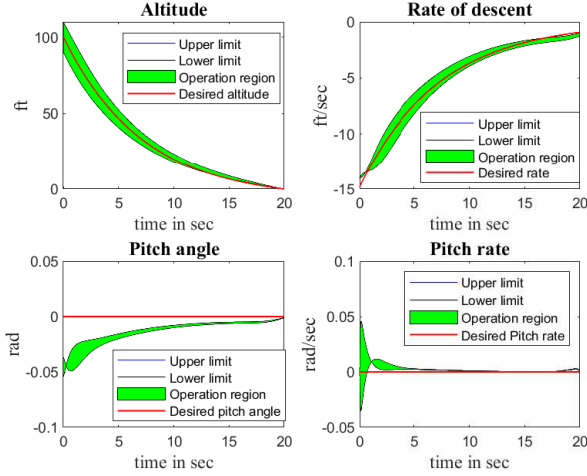


Fig. 8: Trajectory tracking performance for different initial conditions of the flare-out phase.

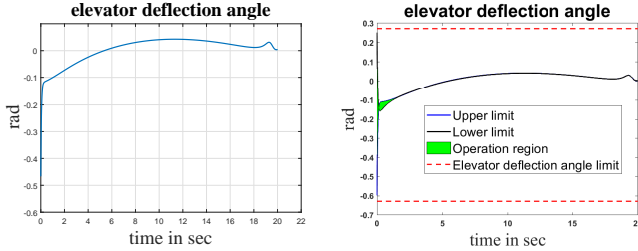


Fig. 9: The control input signal for the flight simulation results for case I (left) and case II (right).

V. CONCLUSION

In this paper, a smooth trajectory tracking system was designed for a fixed-wing aircraft landing. The aircraft landing problem was converted to a finite-time LQT problem. Information on the approach plate of the runway was employed to design a desired smooth landing trajectory. We considered multiple performance requirements and constraints to design an optimal controller which minimizes the trajectory tracking error. The designed controller gives an accurate tracking performance for the flare-out phase of aircraft landing. The simulation result demonstrated the finite-time convergence of the trajectory tracking error. Moreover, the robustness of the designed controller was evaluated against different initial conditions due to the headwind disturbances. This work can be extended by employing a nonlinear model of an aircraft in the presence of turbulent crosswinds and system

uncertainties.

ACKNOWLEDGMENT

This research is supported by Air Force Research Laboratory and OSD under agreement number FA8750-15-2-0116.

REFERENCES

- [1] U. Aviation, "Airplane flying handbook," volume FAA-8083-3A. US Government Printing Office, Washington DC, Tech. Rep., 2004.
- [2] F. Ellert and C. Merriam, "Synthesis of feedback controls using optimization theory—an example," *IEEE Transactions on Automatic Control*, vol. 8, no. 2, pp. 89–103, 1963.
- [3] J.-G. Juang and H.-K. Chiou, "Hardware implementation of aircraft landing controller by evolutionary computation and dsp," *IFAC Proceedings Volumes*, vol. 41, no. 2, pp. 170–175, 2008.
- [4] A. K. Tripathi, V. V. Patel, and R. Padhi, "Autonomous landing of fixed wing unmanned aerial vehicle with reactive collision avoidance," *IFAC-PapersOnLine*, vol. 51, no. 1, pp. 474–479, 2018.
- [5] S.-P. Shue and R. K. Agarwal, "Design of automatic landing systems using mixed h/h control," *Journal of Guidance, Control, and Dynamics*, vol. 22, no. 1, pp. 103–114, 1999.
- [6] M. Lungu and R. Lungu, "Application of h_2/h_∞ technique to aircraft landing control," *Asian Journal of Control*, vol. 17, no. 6, pp. 2153–2164, 2015.
- [7] P. Wu, M. Voskuil, M. Van Tooren, and L. Veldhuis, "Take-off and landing using ground-based power-simulation of critical landing load cases using multibody dynamics," *Journal of Aerospace Engineering*, vol. 29, no. 3, p. 04015070, 2015.
- [8] D. V. Rao and T. H. Go, "Automatic landing system design using sliding mode control," *Aerospace Science and Technology*, vol. 32, no. 1, pp. 180–187, 2014.
- [9] T. Wagner and J. Valasek, "Digital autoland control laws using quantitative feedback theory and direct digital design," *Journal of Guidance, Control, and Dynamics*, vol. 30, no. 5, pp. 1399–1413, 2007.
- [10] A. K. Tripathi and R. Padhi, "Autonomous landing for uavs using t-mpsp guidance and dynamic inversion autopilot," *IFAC-PapersOnLine*, vol. 49, no. 1, pp. 18–23, 2016.
- [11] B. Prasad B and S. Pradeep, "Automatic landing system design using feedback linearization method," in *AIAA Infotech@ Aerospace 2007 Conference and Exhibit*, 2007, p. 2733.
- [12] M. Lungu and R. Lungu, "Landing auto-pilots for aircraft motion in longitudinal plane using adaptive control laws based on neural networks and dynamic inversion," *Asian Journal of Control*, vol. 19, no. 1, pp. 302–315, 2017.
- [13] R. Lungu, M. Lungu, and L. T. Grigorie, "Automatic control of aircraft in longitudinal plane during landing," *IEEE Transactions on Aerospace and Electronic Systems*, vol. 49, no. 2, pp. 1338–1350, 2013.
- [14] K. Lau, R. Lopez, and E. Onate, "Neural networks for optimal control of aircraft landing systems," in *World Congress on Engineering*, vol. 2, 2007.
- [15] B. L. Stevens, F. L. Lewis, and E. N. Johnson, *Aircraft control and simulation: dynamics, controls design, and autonomous systems*. John Wiley & Sons, 2015.
- [16] F. Liao, J. L. Wang, E. K. Poh, and D. Li, "Fault-tolerant robust automatic landing control design," *Journal of guidance, control, and dynamics*, vol. 28, no. 5, pp. 854–871, 2005.
- [17] R. Niewoehner and I. I. Kaminer, "Design of an autoland controller for a carrier-based f-14 aircraft using h_∞ output-feedback synthesis," in *American Control Conference*, 1994, vol. 3. IEEE, 1994, pp. 2501–2505.
- [18] Z. Guan, Y. Ma, Z. Zheng, and N. Guo, "Prescribed performance control for automatic carrier landing with disturbance," *Nonlinear Dynamics*, vol. 94, no. 2, pp. 1335–1349, 2018.
- [19] S. Singh and R. Padhi, "Automatic landing of unmanned aerial vehicles using dynamic inversion," in *Proceedings of the International Conference on Aerospace Science and Technology*, 2008, pp. 26–28.
- [20] J.-G. Juang and J.-Z. Chio, "Fuzzy modelling control for aircraft automatic landing system," *International Journal of Systems Science*, vol. 36, no. 2, pp. 77–87, 2005.
- [21] R. Lungu and M. Lungu, "Automatic control of aircraft in lateral-directional plane during landing," *Asian Journal of Control*, vol. 18, no. 2, pp. 433–446, 2016.